Purdue University

Purdue e-Pubs

Department of Electrical and Computer Engineering Faculty Publications

Department of Electrical and Computer Engineering

1995

Characterization of photon recycling in thin crystalline GaAs light emitting diodes

M. P. Patkar
Purdue University, School of Electrical Engineering

M. S. Lundstrom
Purdue University, School of Electrical Engineering

Michael R. Melloch
Purdue University, School of Electrical Engineering, melloch@purdue.edu

Follow this and additional works at: https://docs.lib.purdue.edu/ecepubs

Part of the Electrical and Computer Engineering Commons

Characterization of photon recycling in thin crystalline GaAs light emitting diodes

M. P. Patkar, M. S. Lundstrom, and M. R. Melloch

Characterization of photon recycling in thin crystalline GaAs light emitting diodes

M. P. Patkar, M. S. Lundstrom, and M. R. Melloch
School of Electrical Engineering, Purdue University, West Lafayette, Indiana

Gallium arsenide light emitting diodes (LEDs) were fabricated using molecular beam epitaxial films on GaAs substrates and removed by epitaxial lift-off (ELO). Lifted off devices were then mounted on a Si wafer using a Pd/Au/Cr contact layer, which also served as a back surface reflector. Devices were characterized by electrical and optical measurements, and the results for devices on the GaAs substrate were compared to those for ELO devices. ELO LEDs coated with a ZnS/MgF_2 antireflection coating exhibited an optical output that was up to six times that of LEDs on GaAs substrates. At the same time, the measured current-voltage characteristics of the ELO devices displayed a lower $n = 1$ current component. ELO LEDs with efficiencies up to 12.5% were realized. We attribute these results to photon recycling enhanced by the back-surface reflector in the ELO LEDs. The luminescence versus current and current versus voltage characteristics of the LEDs were analyzed to obtain the nonradiative minority carrier lifetimes and the photon recycling factors. The results demonstrate that the measured characteristics are well described by photon recycling theory. ELO LEDs may prove useful for characterizing recombination processes in LEDs, and thin-crystalline structures could provide substantial efficiency enhancements for LEDs and solar cells. © *1995 American Institute of Physics.*

I. INTRODUCTION

The numerous existing and developing applications for two closely related devices, III-V light emitting diode (LEDs) and solar cells, demand improved device efficiencies. For GaAs LEDs, efficiencies are typically low (~2–3%) because most of the emitted spontaneous radiation is total internally reflected at the front surface and eventually reabsorbed in the substrate. By using antireflection (AR) coatings,[1] plastic domes,[2] or by thinning the substrates or completely removing them,[3,4] LED efficiencies from 16% to 26% have been achieved. For GaAs solar cells, efficiencies as high as 29% under concentration have been reported.[5] Most of the efficiency gains during the past decade have resulted from improved material quality and processing techniques using the standard, heteroface cell structure introduced by Hovell and Woodall in 1972.[6] To compete with alternative technologies for terrestrial applications, solar cell efficiencies of 35% or more are needed. In this article, we examine the use of thin crystalline device structures and show that they can enhance the efficiencies of LEDs and solar cells as well as serving as a convenient diagnostic tool for materials and device development.

Removing the substrate should increase the efficiency of both LEDs and solar cells by eliminating the absorption losses in the substrate. Consider a GaAs LED with the substrate removed and a high reflectance contact on the back surface. Photons emitted by spontaneous recombination have a ~2% probability of being emitted through the escape cone at the top surface. Photons that are trapped within the structure by the back surface reflector (BSR) and by total internal reflection at the top surface are eventually reabsorbed. As discussed by Schnitzer, *et al.*,[7] each time the phonon "recycles" it has a ~2% probability of escaping. If the material quality and back surface reflectance are high, photons will recycle many times and have numerous opportunities to escape, so the external quantum efficiency will be enhanced.[7] Lush *et al.* performed photoluminescence (PL) measurements on GaAs double heterostructures with and without an underlying substrate and observed more than an order of magnitude increase in the external PL intensity when the substrate was absent.[8] Thin-crystalline LEDs should display enhanced electrical to optical conversion efficiencies, and thin-crystalline solar cells should display enhanced conversion efficiencies because of the increased open-circuit voltage that would result from the lifetime enhancement caused by photon recycling.[9] Because internal quantum efficiencies close to unity are needed to fully exploit the advantage of photon recycling, this technique tends to be highly sensitive to material quality. Photovoltaic quality GaAs has, however, already demonstrated the required material quality.[8]

This article describes our first efforts to enhance LED and solar cell efficiencies by using thin-crystalline device geometries. GaAs LEDs were fabricated and removed from the substrate by the epitaxial lift-off (ELO) process.[10,11] Devices with and without an underlying GaAs substrate were then characterized by optical and electrical measurements. Efficiency enhancements of up to a factor of six were achieved. (Other workers have recently reported thin-crystalline LEDs fabricated with ELO technology which displayed efficiency enhancements of a factor of three.[12]) By carefully analyzing the electrical and optical measurements, we demonstrate that the device operation can be explained in terms of accepted theories for radiative recombination and photon recycling,[13,14] which supports our hypothesis that the efficiency enhancement is due to photon recycling in the thin-crystalline device structure. Electrical and optical characterization of ELO LEDs is also shown to be a convenient diagnostic tool for examining recombination losses in thin-crystalline solar cells. Conventional analysis would require

n GaAs	>1x10^18 cm^-3	100 nm
n GaAs	1x10^18 cm^-3	100 nm
n-Al0.8Ga0.2As	1x10^18 cm^-3	40 nm
n GaAs	1.0x10^18 cm^-3	200 nm
p GaAs	5.4x10^18 cm^-3	2 μm
p-Al0.2Ga0.8As	1x10^19 cm^-3	50 nm
p-GaAs	5x10^19 cm^-3	100 nm
p-AlAs	1x10^19 cm^-3	10 nm
p-GaAs		~40 nm
20 period superlattice 3 nm Al0.23Ga0.77As/ 3 nm GaAs		
p-GaAs	1x10^19 cm^-3	0.9 μm
p GaAs substrate		

FIG. 1. Film structures for the n/p LEDs. The doping density of the 3000 Å n-GaAs layer was estimated from sheet resistance measurements, and the doping density of the 1 μm p-GaAs region by C-V analysis. Layer thicknesses were deduced from the reflection high energy electron diffraction oscillations during MBE.

measurements under high solar concentration where heating effects are difficult to control.

The techniques used to fabricate ELO LEDs are described in Sec. II, and the electrical and optical characterization of the devices, both on and off the substrates, are discussed in Secs. III and IV. We then present in Sec. V a method for analyzing the measurements to extract photon recycling coefficients and nonradiative lifetimes. Finally, we conclude in Sec. VI by summarizing the results and identifying prospects for further efficiency enhancements.

II. DEVICE FABRICATION

GaAs epilayers were grown on GaAs substrates by molecular beam epitaxy in a Varian GEN II system. The film structure, shown in Fig. 1, is an n on p GaAs diode with carrier confinement and contact cap layers. The n-AlGaAs layer above the n-GaAs "emitter" serves as a minority carrier reflector for holes as well as an optical window for emitted radiation. The AlAs separation layer is required by the ELO process[11] used to separate thin crystalline films from the substrate. The p-AlGaAs layer below the p-GaAs "base" confines minority electrons in the base layer. The mole fraction of this layer was selected to be less than 0.4 to prevent etching by the HF selective etch used to remove the AlAs layer during the lift-off process.

LEDs with dimensions from 8×8 to 560×160 μm^2 were fabricated using conventional photolithographic and wet etching techniques. Front contacts to the n-GaAs consisted of AuGe/Ni/Ti/Au metalization. On some of the devices, a ZnS/MgF$_2$ antireflection (AR) coating was deposited by thermal evaporation. Devices used to extract actual values of lifetimes were not AR coated because the presence of an AR coating on bulk GaAs alters its radiative lifetime.[15] (Photoluminescence measurements for extracting lifetimes are usually done without an AR coating.) After LED fabrication, the wafer was cleaved into pieces.

To remove LEDs from the substrate, we used the ELO technique.[11] Similar work has recently been reported by Pollentier et al.,[12] but few details of the electrical and optical characterization were provided. A key fabrication issue is the back contact to the thin-crystalline devices, which should provide low electrical resistance while maintaining a high optical reflectance. Pollentier et al. evaporated Au on the back surface then annealed the contacts at 425 °C. We designed our process sequence to avoid high temperature steps after the devices were removed from the substrate to minimize damage that could lower minority carrier lifetimes. After removing devices from the substrate, they were mounted on a silicon wafer upon which Cr, Au, and Pd had been evaporated. Pd provides a mechanically strong ohmic contact to GaAs,[16] whereas Au is a good reflector. The use of a thin layer of Pd (3–10 nm) on Au is a compromise designed to take advantage of both these properties.

In addition to the electrical and optical measurements to be described in the following two sections, we also estimated the doping densities of the emitter and base layers. It should be apparent that conventional capacitance-voltage (C-V) profiling, which assumes a one-sided junction, is difficult given the doping densities shown in Fig. 1. To estimate the base doping density, we first estimated the emitter doping by performing sheet resistance measurements of the n^+-GaAs. Reverse biased C-V analysis was then used to estimate the base doping density, which was higher than the emitter doping. The result was $N_A = 5.4 \pm 0.5 \times 10^{18}$ cm^{-3}.

The reflectivity of the Pd/Au metalization was also measured and found to be 75% to 90% at a wavelength of 870 nm (which corresponds to the peak of the emission spectrum of a p-AlGaAs/GaAs double heterostructure). The Pd layer thickness varied from 10 to 3 nm with the lower reflectivities being observed for thicker Pd layers. The thin-crystalline devices analyzed for this work had Pd/Au back surface reflectors with 5.5-nm-thick layers of Pd which gave 85% reflectivity.

III. CURRENT-VOLTAGE CHARACTERIZATION

The diodes' current-voltage (I-V) characteristics were measured before and after ELO; a typical result for an AR coated n/p diode is shown in Fig. 2. While the thin film devices showed somewhat larger leakage currents at low voltages, at the operating voltages ($\geqslant 1$ V) the currents were nearly identical. The thin film devices displayed lower series
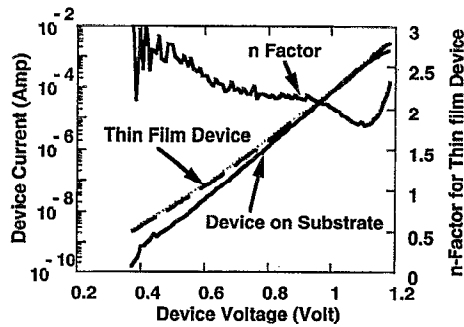
FIG. 2. I-V characteristics of an 80×80 μm^2 LED before and after epitaxial lift-off. The measurement temperature was 23.4 °C. The ideality factor of the ELO device is also shown.

resistances than those on the substrate, which indicates that the Pd layer provided a low resistance contact to the p GaAs. Also shown in Fig. 2 is the diode ideality factor versus bias for a thin film device. The $n \cong 2$ characteristic observed for low bias is expected to be perimeter dominated,[17] and the reduction of n factor at higher biases reflects the increasing importance of the $n = 1$ bulk recombination current.

The measured I-V characteristics of the diodes were analyzed to extract the values of the J_{01} and J_{02} saturation current densities. Table I lists the extracted J_{01} and J_{02} current densities (averaged over five devices that showed good optical efficiencies) for devices without an AR coat. The measurement temperatures were 297 ± 0.5 K. Table I shows that J_{01} decreases by a factor of ~ 3 and the J_{02} value increases slightly for thin film devices as compared to devices on substrates. As discussed below, the decrease in J_{01} was anticipated, but no change in J_{02} was expected. The increase in J_{02} could be due to the use of TCA as a solvent for the wax that coated the samples during the ELO process. Being a chlorinated solvent, TCA could affect the perimeter recombination velocity of the mesa etched devices.

For a one-sided diode dominated by electron injection into the p-type region, the J_{01} saturation current density can be written as

$$J_{01} = \frac{q n_i^2 W}{N_A} \left(\frac{1}{\Phi \tau_r} + \frac{1}{\tau_{nr}} + \frac{S}{W} \right),$$ (1)

where n_i is the intrinsic carrier concentration in the base, N_A is the base doping density, W the width of the base, τ_r and τ_{nr} the radiative and nonradiative lifetimes, Φ the photon recycling factor,[13] S the recombination velocity at the GaAs/AlGaAs interface, and W is the width of the base. Equation

(1) is derived by assuming that there is no injection of carriers from base to emitter and that the minority carrier diffusion length is much longer than the base width W.

Given the doping densities displayed in Fig. 1, the validity of Eq. (1) must be questioned. The heavier doping in the p base suggests that the hole current injected into the emitter will be more than five times the electron current injected into the base. Much of this difference, however, is offset by the fact that the emitter is less than one-third the thickness of the base. In addition, effective bandgap narrowing effects increased n_i in the base and decreased it in the emitter.[18] The lower radiative lifetime in the base also acts to increase the base current component. When these factors are included, we estimate the ratio of the carrier injection into the base to the back injection into the emitter to be about 6.5:1. This estimate shows that although the base doping is higher than the emitter doping, Eq. (1) accounts for about 85% of the $n = 1$ current.

According to Eq. (1), the measured decrease in J_{01} indicates that the lift-off process not only did not significantly damage the devices but actually increased the effective radiative lifetime. Such an increase is expected if so-called photon recycling effects are enhanced in thin-crystalline films [which increases the recycling factor, Φ in Eq. (1)]. Enhanced minority carrier lifetimes attributed to photon recycling have recently been observed by Lush *et al.* in thin-crystalline AlGaAs/GaAs double heterostructures.[8] In that case, lifetime enhancements of a factor of 10 were observed. The factor of 3 reduction in J_{01} indicates that the effective radiative lifetimes in the thin-crystalline cells is about three times that before they were removed from the GaAs substrate.

IV. OPTICAL CHARACTERIZATION

Measurements were also performed to characterize the optical output as a function of the device current. Devices were probed while a calibrated Si detector was placed as close to the device as possible. Current pulses with a duty cycle of 2 μs/1000 μs were applied, and the output of the detector was measured using an Oriel 7070 radiometer. Devices with optical emitter sizes of 80×80 and 120×120 μm^2 gave the best results because they were small enough to pump to high current densities (> 1000 A/cm^2) and their resistances were small so they suffered less from heating effects at high current densities. Figure 3 shows a comparison of the optical outputs from a 120×120 μm^2 device with an AR coat before and after liftoff. The output of the thin film device is seen to be about five times that of the device on the GaAs substrate, which can be attributed to the effects of optical confinement and photon recycling that occur in GaAs thin films mounted on back surface reflectors. Devices without an AR coat showed an enhancement of optical output by a factor of ~ 2.5 when the ELO devices were compared to those on the GaAs substrate. Devices with an AR coating were expected to display higher optical output, but the increased improvement factor after removing the substrate was not expected. One possibility is that pinholes in the AR coat-

TABLE I. Saturation current densities deduced from dark current vs voltage measurements before and after epitaxial liftoff. J_{01} is averaged over six devices, and J_{02} is averaged over only the 120×120 μm^2 devices. The devices did not have an antireflection coating.

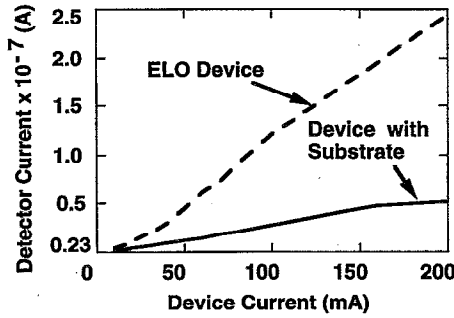| Device	$J_{01}(\times 10^{-20}$ A/cm$^2)$	$J_{02}(\times 10^{-10}$ A/cm$^2)$ (for 120×120 μm^2 devices)
Before ELO	4.14	8.0
After ELO	1.41	13.5

FIG. 3. Comparison of the optical output of a 120×120 μm^2 device before and after epilayer lift-off. The measurement temperature was 23.6 °C.

ing may have effectively texturized the front surface thereby enhancing the optical output by the mechanism discussed by Schnitzer et al.[19]

The efficiencies of the LEDs were estimated as follows.[20] The emitted radiation pattern was found to be Lambertian, so the total optical output of the LED is

$$I_L = I_{\text{Det}} \times f \times \frac{\pi r^2}{A_{\text{Det}}} \times \frac{S_F}{S_{\text{Det}}}, \qquad (2)$$

where I_L is the total number of photons emitted per second, I_{Det} is the detector current, f is the inverse of the duty cycle, r is the distance from the detector to the LED, A_{Det} is the area of the detector, S_F is the shadowing correction for the area of the LED shadowed by the grid, and S_{Det} is the sensitivity of the detector (number of electrons collected for each photon incident on the detector).

The external efficiency of the LEDs was calculated from

$$\eta_{\text{ext}} = \frac{I_L}{I_D}, \qquad (3)$$

where I_L is obtained from Eq. (2) and the measured detector current, and I_D is the measured device current corresponding to I_L.

Figure 4 plots the normalized LED efficiency and the current ratio $I_{n=1}/I_D$ vs I_D for a 120×120 μm^2 device. The LED efficiency increases rapidly at first and then levels off at currents greater than about 100 mA. To evaluate the $(I_{n=1}/I_D)$ ratio, the $n=1$ and $n=2$ saturation currents were
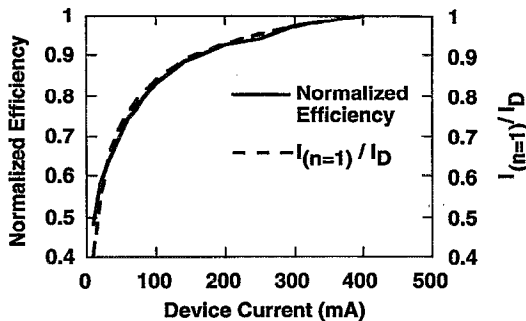

FIG. 4. $(I_{n=1}/I_D)$ vs I_D for a 120×120 μm^2 ELO LED. Also plotted is the normalized external quantum efficiency, $\eta_{\text{ext}}/\eta_{\text{ext}}$ (max).

extracted from the measured I-V characteristics of the devices, and we assumed that $I_D = I_{n=1} + I_{n=2}$ (which neglects the small leakage current). Figure 4 shows that the efficiency versus I_D characteristic closely matches the $(I_{n=1}/I_D)$ ratio. The efficiency is initially low when I_D is dominated by the nonradiative $n=2$ current and finally saturates for $J_{\text{Total}} \geqslant 520$ A/cm^2 when the diode current is dominated by the $n=1$ recombination currents. Maximum efficiencies ranging from 6% to 12.5% were achieved for the AR coated LEDs at 1041 A/cm^2. From Fig. 4, we observe that the $(I_{n=1}/I_D)$ ratio is approximately 93% at a current of 200 mA (a current density of ~1400 A/cm^2 for these 120×120 μm^2 devices).

Because the I_L vs I_D characteristic closely follows the $(I_{n=1}/I_D)$ vs I_D characteristic, it provides a convenient means of estimating the $n=1$ current component. As shown in Fig. 2, the $n=2$ current is easy to extract, because the I_D vs V characteristic is dominated by the $n=2$ current over a wide voltage range. The $n=1$ current, however, can be difficult to extract, especially for high quality devices in which the $n=1$ current is small. As shown in Fig. 4, however, the shape of the $(I_{n=1}/I_D)$ vs I_D characteristic is determined by both the $n=1$ and $n=2$ current components. By plotting $I_{n=1}/(I_{n=1}+I_{n=2})$ vs I_D using the value of $I_{n=2}$ extracted from the I_D vs V characteristic and adjusting the $I_{n=1}$ current until the shape of the characteristic matches the I_L vs I_D characteristic, an accurate value for $I_{n=1}$ can be deduced.

V. ANALYSIS

The current versus voltage and intensity versus current measurements were used to estimate the nonradiative minority carrier lifetimes and the photon recycling factors in the p-type base regions of the LEDs as follows. We begin with an expression similar to one given by Schnitzer et al.[19] that relates the external and internal quantum efficiencies,

$$\eta_{\text{ext}} = \eta_{\text{int}} \times \left(\frac{I_{n=1}}{I_D} \right) \times \frac{\bar{T}/4n^2}{\bar{T}/4n^2 + (1 - \eta_{\text{int}}) + L/4\alpha_0 d_0}, \qquad (4)$$

where α_0 is the absorption coefficient of the active layer, d_0 is the thickness of the active layer, η_{int} is the internal (radiative) quantum efficiency, n is the refractive index of the active layer, $\bar{T}$ is the wavelength-averaged optical transmission coefficient at the GaAs/air interface for normal incidence (70%), and L is a loss term that includes the losses by absorption at the BSR and in the window and cap layers of the device. The loss term is given by

$$L = (1 - \bar{R}) + 4\Sigma \alpha_i d_i, \qquad (5)$$

where, α_i and d_i are the absorption coefficients and thicknesses respectively of the parasitic layers in the LED structure, and $\bar{R}$ is the angle averaged reflectivity of the BSR.

The term

$$\frac{\bar{T}/4n^2}{\bar{T}/4n^2 + (1 - \eta_{\text{int}}) + L/4\alpha_0 d_0}$$

in Eq. (3) represents the ratio of the amount of optical radiation emitted by the device to the total loss of optical radiation within the device.[19] The efficiency, which is the ratio of the

optical output of the LED to the total current input to the LED, is given by the above mentioned term multiplied by the internal quantum efficiency (because internal quantum efficiency represents the fraction of the $n = 1$ bulk recombination that occurs radiatively) and the $(I_{n=1}/I_D)$ ratio, which finally results in Eq. (4).

To estimate the internal quantum efficiency, η_{int}, from the measured LED efficiency, η_{ext}, we make use of Eq. (4). We first calculated the $(I_{n=1}/I_D)$ ratio using the values for J_{01} and J_{02} extracted from the current versus voltage analysis. The LED current, I_D, was selected so that the device was not influenced by heating. Using the measured value for $\bar{R}$ and available data for the absorption coefficients of n- and p-type GaAs,[21,22] the term $L/4\alpha_0 d_0$ was calculated. Substituting the measured value of η_{ext}, the computed values of $(I_{n=1}/I_D)$ and $L/4\alpha_0 d_0$ into Eq. (4), we finally deduce η_{int}.

The internal radiative quantum efficiency, η_{int}, in the base of the LEDs is given by

$$\eta_{int} = \frac{\tau'_{nr}}{\tau'_{nr} + \tau_r},\qquad(6)$$

where τ_r is the radiative lifetime in the active region of the LED, and τ'_{nr} is given by

$$\frac{1}{\tau'_{nr}} = \frac{1}{\tau_{nr}} + \frac{S}{W},\qquad(7)$$

with S being the surface recombination velocity at the GaAs/AlGaAs interface and W the width of the active region. The radiative lifetime is

$$\tau_r = \frac{1}{BN_A},\qquad(8)$$

where $B = 2 \times 10^{-10}$ cm^3/s as computed by Casey and Stern.[23] From the estimated base doping density of 5.4×10^{18} cm^{-3}, we find $\tau_r = 0.9$ ns. Using this value of τ_r and the value of η_{int} obtained from Eq. (4), an estimate of τ'_{nr} is obtained from Eq. (6). We also have available from the measured I-V characteristic the $n = 1$ saturation current density,

$$J_{01} = \frac{qn_i^2 W}{N_A}\left(\frac{1}{\Phi\tau_r} + \frac{1}{\tau'_{nr}}\right).$$

With the value for $qn_i^2 W/N_A$ computed from the doping-dependent n_i (Ref. 18) at the same temperature at which J_{01} was measured, we estimate the value of $1/\Phi\tau_r + 1/\tau'_{nr}$. Finally, with the previously estimated value of τ'_{nr}, a value for Φ is obtained. The same procedure was used to calculate lifetimes in the bases of LEDs on the substrate. The back surface reflectance was taken to be 55%, which accounts for the reflectance of the GaAs/AlGaAs interface.

Table II summarizes the results of the calculations. The devices on substrates without an AR coat exhibited an average photon recycling factor of 2.5. The ELO devices without an AR coat exhibited an average photon recycling factor of 6.6, about 2.8 times that exhibited by the devices on substrates. This is consistent with the factor of 2.5 increase in the optical output of the LEDs after they were removed from the substrate. Recall that the average value of J_{01} decreased by factor of 2.9. All of these observations are consistent with

TABLE II. Photon recycling factors and nonradiative lifetimes for LEDs with and without an underlying substrate. The devices did not have an antireflection coating.

Device	Φ	τ'_{nr} (ns)	Upper limit S (cm/s)
Before ELO	2.5	16.0	1.25×10^4
After ELO	6.6	9.9	2×10^4

an enhancement in carrier lifetime caused by increased photon recycling in the thin-crystalline LEDs. Theoretically calculated values for the photon recycling coefficient are ~3.3 for a device on substrate and 6.3 for a thin film device. Given the estimated error bars in the experimentally deduced photon recycling coefficients (about -20% to $+29\%$), it appears that the experimental values for Φ compare well with conventional photon recycling theory.[13,14]

Turning now to the nonradiative lifetimes, it should be noted that it is not possible to separate S from τ_{nr} in this analysis, but we can place upper limits on S and lower limits on τ_{nr}. For devices on substrates, the upper limit on S was estimated to be 1.25×10^4 cm/s and for thin crystalline devices, 2×10^4 cm/s. Interface recombination velocities at the $Al_{0.3}Ga_{0.7}As$/GaAs interface are expected to be much lower than these upper bounds. Assuming $S = 0$, we find the lower bounds on τ_{nr} to be 16 ns for devices on the substrate and 10 ns for ELO devices. Thus, we find nonradiative lifetimes that are more than ten times the radiative lifetimes, which should permit significant photon recycling. The nonradiative lifetimes in the thin-film devices are less than those for the devices on substrates by about 35%. The estimated error in the nonradiative lifetimes is about 25%, so the ELO process may have produced some slight damage to the films, but this is far from clear.

Finally, it is interesting to project the efficiencies that might be obtained in high lifetime samples with optimized designs. The thin crystalline devices showed an η_{int} of about 91%. Internal quantum efficiencies greater than 99% have been demonstrated in thin-film GaAs/AlGaAs double heterostructures grown by metal-organic chemical-vapor deposition.[8] Using Eq. (4), we project an efficiency of about 15% for thin-film LEDs with values of η_{int} of 99% and $(I_{n=1}/I_D)$ of 95%, $\bar{T}$ equal to 100% (diodes with a perfect AR coat), and a back surface reflectance of 97%. This relatively low projected efficiency is an indication that the structures are limited by parasitic absorption in the relatively thick contact cap layers of the LED. If the thicknesses of these layers are reduced to 150 Å, the projected efficiency rises from 15% to about 27%.

VI. CONCLUSIONS

LEDs were fabricated, removed from the substrate by the epilayer lift-off technique, and their electrical and optical performance characterized in detail. ELO diodes with an antireflection coating showed an optical output that was up to six times larger than the output of the same device when on the substrate. We attribute this increase in performance to optical confinement and photon recycling in ELO GaAs

LEDs mounted on a back surface reflector. The use of thin crystalline structures with back surface reflectors has previously been proposed as a means of lowering the threshold current of a semiconductor laser;[10] our work demonstrates that similar benefits can be achieved for LEDs. LED efficiencies of up to 12.5% at current density of 1041 A/cm^2 were achieved. To achieve higher efficiencies, losses in the electrically inactive regions of the LED need to be reduced, and for ultimate efficiencies, improved minority carrier lifetimes will be necessary.

From the detailed optical and electrical characterization of the LEDs, the nonradiative minority carrier lifetimes and photon recycling factors were estimated. The increase in the photon recycling factors after devices were removed from the substrate presents clear evidence of photon recycling. These simple measurements may prove useful as a diagnostic tool for evaluating minority carrier lifetimes, photon recycling factors, and for extracting small $n = 1$ saturation current densities. Such measurements would provide a convenient means for examining various device structures for single junction high-efficiency solar cells and LEDs. Because of the close relationship between the electrical to optical conversion efficiency of an LED and the optical to electrical conversion efficiency of a solar cell,[25] high-efficiency LED structures should also serve as high-efficiency solar cells.

ACKNOWLEDGMENT

[1] H. Rupprecht, J. M. Woodall, K. Konnerth, and D. G. Pettit, Appl. Phys. Lett. 9, 221 (1966).
[2] I. Ladany, J. Appl. Phys. 42, 654 (1971).
[3] C. A. Burus and R. W. Dawson, Appl. Phys. Lett. 17, 97 (1970).
[4] S. Wang, Fundamentals of Semiconductor Device Theory (Prentice Hall, Englewood Cliffs, NJ, 1989), p. 755.
[5] N. R. Kaminar, D. D. Liu, H. F. MacMillan, L. D. Partain, M. Ladle Ristow, and G. F. Virshup, Appl. Phys. Lett. 17, 97 (1970).
[6] H. Hovel and J. M. Woodall, Conf. Rec. 21st IEEE Photovoltaic Spec. Conference, 1972, p. 766.
[7] I. Schnitzer, E. Yablonovich, C. Canau, and T. Gmitter, Appl. Phys. Lett. 62, 131 (1993).
[8] G. B. Lush, M. R. Melloch, M. S. Lundstrom, D. H. Levi, R. K. Ahrenkiel, and H. F. MacMillan, Appl. Phys. Lett. 61, 2440 (1992).
[9] G. B. Lush and M. S. Lundstrom, Solar Cells 30, 337 (1991).
[10] F. Stern and J. M. Woodall, J. Appl. Phys. 45, 3904 (1974).
[11] E. Yablonovich, T. Gmitter, J. P. Harbison, and R. Bhat, Appl. Phys. Lett. 51, 2222 (1987).
[12] I. Pollentier, A. Ackaert, P. De Dobbelaere, L. Buydens, P. Van Daele, and P. Demester, SPIE 1361 Physical Concepts of Materials for Novel Optoelectronic Device Applications, 1990, p. 1056.
[13] R. K. Ahrenkiel, Semiconductors and Semimetals (Academic, Boston, MA, 1993), Vol. 39, Chap. 2, p. 40.
[14] D. Z. Garbuzov, in Semiconductors Physics, edited by V. M. Tuchkervich and V. Ya. Frenkel (Consultants Bureau, New York, NY, 1988).
[15] E. Yablonovich, T. J. Gmitter, and R. Bhat, Phys. Rev. Lett. 61, 2546 (1988).
[16] E. Yablonovich, T. Sands, D. M. Huang, I. Schnitzer, and T. Gmitter, Appl. Phys. Lett. 59, 3159 (1991).
[17] T. Stellwag, M. R. Melloch, M. S. Lundstrom, M. S. Carpenter, and R. F. Pierret, Appl. Phys. Lett. 56, 1658 (1990).
[18] E. S. Harmon, M. R. Melloch, and M. S. Lundstrom, Appl Phys. Lett. 64, 502 (1994).
[19] I. Schnitzer, E. Yablonovich, C. Canau, T. J. Gmitter, and A. Scherer, Appl. Phys. Lett. 63, 2174 (1993).
[20] H. Jeon, J. Ding, A. V. Nurmikko, W. Xie, M. Kobayashi, and R. L. Gunshor, Appl. Phys. Lett. 60, 892 (1992).
[21] G. B. Lush, H. F. MacMillan, S. Asher, M. R. Melloch, and M. S. Lundstrom, J. Appl. Phys. 74, 4684 (1993).
[22] H. C. Casey Jr., D. D. Sell, and K. W. Wecht, J. Appl. Phys. 46, 250 (1975).
[23] H. C. Casey, Jr. and F. Stern, J. Appl. Phys. 47, 631 (1976).
[24] G. B. Lush, Ph.D thesis, School of Electrical Engineering, Purdue University, West Lafayette, Indiana, 1992, p. 75.
[25] G. Smestad and H. Ries, Sol. Energy Mater. Sol. Cells 25, 51 (1992).

Published without author corrections

RIGHTSLINK()